Production of PEG grafted PAN copolymers and Their Electrospun Nanowebs as Novel Thermal Energy Storage Materials

Nihal Sarier[1*], Refik Arat[1], Yusuf Menceloglu[2], Emel Onder[3], Ezgi Ceren Boz[3], Oguzhan Oguz[2]

[1] *Istanbul Kultur University, Faculty of Engineering, 34156 Bakirkoy, Istanbul, Turkey*

[2]*Sabanci University, Faculty of Engineering and Natural Sciences,34956 Tuzla, Istanbul,Turkey*

[3]*Istanbul Technical University, Faculty of Textile Technologies and Design, 34437Gumussuyu, Istanbul,Turkey*

**Corresponding AuthorPhone: +90 212 4984258; Fax: +90 2124658308; E-mail address: n.sarier@iku.edu.tr*

Highlights of Production of PEG grafted PAN copolymers and Their Electrospun Nanowebs as Novel Thermal Energy Storage Materials

- PEG-g-PAN copolymers were synthesized successfully as novel solid-solid PCMs.
- PEG-g-PAN copolymers display phase change at 40–65 ^{o}C by absorbing and releasing 70–126 Jg^{-1} heat.
- The nanowebs, produced by coaxial electrospinning, were composed of hollow PEG-g-PAN nanofibers with 175–277 nm diameters.
- PEG-g-PAN nanowebs can be used as dynamic thermal energy storage materials in industry.

Abstract

This paper deals with the synthesis of poly(ethylene glycol) (PEG) grafted poly(acrylo nitrile) (PAN) copolymers as novel solid-solid phase change materials via two step free radical polymerization reaction. The structural and thermal characterizations of the synthesized copolymers, namely PEG1500-g-PAN, PEG2000-g-PAN, PEG4000-g-PAN, PEG10000-g-PAN and PEG35000-g-PAN, were performed by Fourier transform infrared spectroscopy, Nuclear magnetic resonance spectrometry, differential scanning calorimetry and thermogravimetry. They were thermally stable and had the capability of absorbing and releasing great amount of heat ranging between 70 and 126 Jg^{-1} at the temperature interval of 40–65 ^{o}C during heating and successive cooling cycles. To transform the PEG-g-PAN copolymers into the assemblies appropriate for thermal energy storage (TES) systems, thermo-regulating PEG-g-PAN nanowebs were also produced by means of coaxial electrospinning. The SEM images of PEG-g-PAN nanowebs displayed that they were all composed of hollow cylindrical ultrafine fibers with the average diameters ranging in 175–277 nm. During the differential scanning calorimetry measurements, those nanowebs demonstrated repeatable solid-solid phase change with the heat storage capacities varying between 35 and 75 Jg^{-1} at the same temperature interval with the corresponding PEG-g-PAN copolymers. The PEG-g-PAN copolymers and their electrospun nanowebs can be promising TES materials and can have convenient industrial applications.

Key words: PCM, PEG, PAN, grafting, electrospinning, DSC.

1 Introduction

Solid-solid phase change materials (SSPCMs) are crystalline solids that undergo phase changes from one lattice configuration to another by absorbing and releasing great amount of latent heat at well-defined temperatures below their melting points. The SSPCMs originate their remarkable performance from their configuration and the physical bonding that occurs between neighboring molecules in the crystalline solid [1] and [2]. At low temperatures, the intermolecular physical attractions restrict molecular movement. At the phase transition temperature, a SSPCM absorbs an amount of energy and the physical bonds break, allowing the molecules to rotate and vibrate more freely in their lattice sites. When the material is cooled, the intermolecular physical bonds rebuild and the same amount of heat is released. The magnitude of physical attractions mainly affects the amount of energy absorbed and released throughout the solid-solid phase transition. By combining molecules of different structure in the same crystalline solid, the strength of physical bonding can be altered, thus phase transition temperature interval and heat storage capacity of a SSPCM can be modified [1], [2] and [3]. SSPCMs can be a good alternate for the solid–liquid PCMs in various thermal energy storage (TES) applications. The most attractive properties of SSPCMs can be listed as high enthalpy of phase change, suitable phase change temperature interval for practical applications, chemical and thermal stability, small volume change, no segregation and leakage during phase change, safe and convenient handling, compatibility with a lot of polymers, and non-toxicity [1], [2], [3], [4], [5], [6], [7], [8], [9] and [10].

Poly(ethylene glycol)s (PEGs), composed of repeating linear dimethyl ether chains with hydroxyl ending groups, have gained a considerable interest in the production of SSPCMs, owing to their high latent heat of solid-liquid phase change in diverse temperature ranges, good thermal cycling ability, high crystallinity and capability of making intermolecular hydrogen bonding and of undergoing polymerization reactions. Nowadays, a number of research groups has reported the successful syntheses of various PEG based copolymers such as polypropylene-*graft*-PEG [10], cellulose diacetate-*graft*-PEG [12], [13],

polystyrene-*graft*-PEG[14], polyurethane-*graft*-PEG [15] and [16], cellulose-*graft*-PEG [17], poly(vinyl alcohol)-*graft*-PEG [18], polyethylene terephalate-*graft*-PEG copolymers [19], and cellulose-*graft*-PEG[20] by means of graft copolymerization technique where PEG chains functioning as the soft segment and other constituents serving as the hard segment of a copolymer. Most of those PEG based copolymers have considerable enthalpies so long as the molecular weights of PEGs are equal to or greater than 4000 $gmole^{-1}$ [21] and [22].

Poly(acrylonitrile) (PAN), on account of its solvent resistance, chemical and thermal stability, high tensile strength and good pest resistance, has been widely used in the consumer products like textile fibers, drinking cups, automotive parts and appliances [23]. Regardless of reputation of PAN in industrial applications, to the best of our knowledge, only limited reports specified the production of PCM-PAN copolymers as SSPCMs. Guo et al. prepared PEG4000-PAN copolymer as SSPCM having the phase transition enthalpy of 74 Jg^{-1} at 52 °C, by the aqueous phase precipitation polymerization [24]. Recently, Mu et al. grafted PEG4000 to the chain of poly(styrene-co-acrylonitrile) to produce SAN-g-PEG copolymer with the phase transition at 36 °C and the latent heat of 68 Jg^{-1} [25]. Very recently, Mu et al. synthesized poly(acrylonitrile-co-itaconate)-*graft*-PEG4000 copolymer, having the thermal energy absorption capacity of 70 Jg^{-1} at 53 °C [26].

In general, not only the production of PCMs but also their incorporation into TES systems has attracted increasing attention owing to the thermal and physical requirements for the final product, such as high thermal insulation capability, thermal stability, durability and flexibility. In this manner, a number of research groups has focused on the production of thermally improved fibres by different approaches such as filling hollow fibres with PEGs [27] and [28], melt or wet spinning of PEG-polymer mixtures [29], [30] and [31], grafting of PEGs onto fibers [20], and recently electrospinning of PEG-polymer mixtures [32], [33], [34] and [35] for the manufacture of heat-storage and thermo-regulated composites[36]. In the matter of SSPCMs, the research studies related with the integration of SSPCMs to fibre, fabric or foam structures are restricted. Very recently, Zhang et al. reported the

electrostatic spinning of as produced poly(acrylonitrile-*co*-acrylamide)-*g*-PEG4000 copolymers [37]. The research in the manufacture and effective incorporation of SSPCMs to the dynamic thermal insulation products seem to spread progressively.

In the present study, we first synthesized PEG-g-PAN copolymers as novel SSPCMs by grafting PEG1500, PEG2000, PEG4000, PEG10000 and PEG35000 oligomers with polyacrylonitrile chains through two step free radical copolymerization reactions. We then produced new types of thermo-regulating nanowebs, composed of hollow nanofibres of PEG-g-PAN by means of coaxial electrospinning for transforming the synthesized PEG-g-PAN copolymers into the assemblies appropriate for numerous industrial areas such as textiles, packaging, solar energy systems, building envelopes and biomedical materials. The structural and thermal characterizations of PEG-g-PAN copolymers as well as those of the electrospun nanowebs were performed in detail.

2 Experimental

2.1 Materials:

Poly(ethylene glycol)s (PEGs) with the molecular weights of 1500 $gmole^{-1}$ (PEG1500), 2000 $gmole^{-1}$ (PEG2000), 4000 $gmole^{-1}$ (PEG4000), 10000 $gmole^{-1}$ (PEG10000) and 35000 $gmole^{-1}$ (PEG35000), Maleic anhydride (MAH), Acrylonitrile (AN), p-Toluene sulphonic acid (PTSA), Azobisisobutyronitrile (AIBN), Dimethyl acetamide (DMAc) and the other chemical reagents, purchased from Sigma-Aldrich Inc., were all technical grade and used for the synthesis of PEG-g-PAN copolymers without further purification.

2.2 Synthesis of PEG-g-PAN copolymers

Prior to grafting reactions, poly(ethylene glycol) (PEG) oligomers of different molecular weights were submitted to transesterification reaction with maleic anhydride (MAH) to obtain more reactive macromonomers of PEG-MA [36]. The steps of transesterification reaction between PEG and MAH are shown in Fig. 1, and the reaction ingredients are summarized in Table 1, correspondingly.

In a three-necked round-bottomed flask equipped with a magnetic stir bar and reflux condenser, stoichiometric amounts of PEG and MAH were mixed and heated to 60°C under a slightly positive nitrogen atmosphere while stirring at 1000 rpm for 30 min. Then PTSA, which was 1% by mole of MAH, was added into the reaction mixture as a catalyst. The flask temperature was then raised to 90°C and refluxed for 3 h at 1000 rpm. After cooling to room temperature, the reaction mixture was precipitated in hexane (100 mL) and filtered. The filter cake of PEG-MA macromonomer was washed in excess hexane for purification, and then dried overnight in a petri dish.

After preparation of PEG-MA macromonomers, the syntheses of PEG-g-PAN copolymers by free radical polymerization were performed [38]. Amounts of ingredients to produce PEG-g-PAN copolymers via free radical copolymerization are summarized in Table 2.

The known amount of PEG-MA was dissolved in 25 mL dimethyl acetamide (DMAc) in a three-necked round-bottomed flask in an oil bath at 70^{o}C. The equivalent amount of AN monomer was then slowly injected into the flask under nitrogen atmosphere while stirring at 500 rpm for 30 min. Under given conditions, the initiator AIBN, which was 1% by mass of AN, was added slowly to the reaction mixture. The copolymerization reaction between PEG-MA ester and AN was carried out at temperature of 70 ^{o}C for 24 h under inert nitrogen atmosphere while stirring the system at 500 rpm. Grafting of PEG-MA with AN by a free radical polymerization is as given in Fig. 2.

The PEG-g-PAN copolymers were obtained as yellowish white precipitate at the bottom of the reaction vessel. After cooling to room temperature, each product mixture was 3–4 times reprecipitated in 3 volume ethanol-1 volume hexane mixture to remove unreacted residues. The rewashed and recrystallized PEG-g-PAN copolymer was then dried in vacuum on a

rotary evaporator at room temperature and stored in a closed glass bottle. The pristine PAN was also synthesized under the same reaction conditions and labeled as PAN control.

2.3 Preparation of electrospun PEG-g-PAN hallow nanofibers

In the second part of the study, nanowebs made up of electrospun PEG-g-PAN hallow nanofibers were produced.

2.3.1 Preparation and characterization of shell solutions used in electrospinning

To produce electrospun hollow nanofibers, the shell solution was prepared as a mixture of commercial poly(acrylo nitrile) (PAN) and synthesized PEG-g-PAN copolymers both dissolved in DMAc. The poly(acrylo nitrile) (PAN) with the average molecular weight of 150,000 $gmol^{-1}$ and the density of 1.18 gcm^{-3}, supplied from Good Fellow Corp. (GB), was preferred considering its suitability for the manufacture of ultra-fine fibres in engineering applications [39] and [40]. Each of 10% PEG-g-PAN (by weight) solutions and 6% PAN (by weight) solution were dissolved in DMAc by stirring at 500 rpm under ambient conditions for 2 hours. Then, they were mixed in one to one ratio by volume to obtain a shell solution suitable for electrospinning. The kinematic viscosity measurements of shell solutions were carried out with Ubbelohde viscometer at 25 °C following the standard capillary method ASTM D445 [41]. The surface tensions of solutions were measured with a Neubert Glass model Traube Stalagmometer following the method given in the literature [42]. The stalagmometer volume was 2.5 mL and the reference liquid was taken as water at 25^{o}C. The surface tensions were averaged over five measurements. The electrical conductivity measurements of shell solutions were performed at 25^{o}C, using Mettler Toledo S80 model Multi Conductometer between 0.001 μScm^{-1} and 1000 $mScm^{-1}$. The conductometer was calibrated with the standard solution (84 $\mu Siemenscm^{-1}$) and the cell constant was taken as ≤ 0.1.

2.3.2 Coaxial electrospinning of PEG-g-PAN and PAN mixtures

Electrospinning experiments were performed using the coaxial electrospinning device, Yflow Co. (Spain) [43], with 15 cm collector distance at a voltage value between 14 and 16 kV for 60 minutes at 25 ºC. The spinneret of the device consists of two stainless-steel coaxial needles with outer diameters (ODs) of 0.9 and 1.7 mm, and inner diameters (IDs) of 0.6 and 1.4 mm, respectively, connected to a reservoir. The shell mixture was pumped through the outer injector of the electrospinning device at a certain speed while the air was pumped through the inner injector. Optimized coaxial electrospinning parameters were ensured for each case when the Taylor cone anchored at the tip of the nozzle was watched by the Taylor cone visualization system of the device. The conditions for the production of PEG-g-PAN nanowebs and 6PAN nanoweb (control) are presented in Table 3.

2.4 Characterization of PEG-g-PAN copolymers and electrospun PEG-g-PAN nanowebs

The Fourier Transform Infrared (FTIR) transmission spectra of the synthesized copolymers as well as those of electrospun nanowebs were recorded between 4000−650 cm^{-1} at a resolution of 4 cm^{-1} by a Perkin Elmer Spectrum 100 FTIR spectrometer equipped with a universal attenuated total reflection (ATR) accessory. 1H and 13C Nuclear Magnetic Resonance (NMR) spectra of all the PEG-g-PAN specimens were recorded on a BRUKER AVANCE III 500 MHz spectrometer operating at 500.13 MHz for 1H experiments and 125.77 MHz for 13C experiments, equipped with a 5 mm dual-resonance BBO probe incorporating gradients for the z-axis (Bruker Bio Spin GmbH, Germany). Chemical shifts (δ) were reported in the units of ppm and referenced to the solvent 13C resonances in deuterated solvents. The polymer solutions with the concentrations of 15 $mgmL^{-1}$ for 1H-NMR test and of 44 $mgmL^{-1}$ for 13C-NMR test were prepared by mixing with analytical grade dimethyl sulfoxide (DMSO) at room temperature.

Thermal properties of all the samples were examined by a Perkin Elmer DSC 4000 differential scanning calorimeter with an accuracy of ±0.001. A nitrogen flux (20 $mLmin^{-1}$) was used as a purge gas for the furnace. Temperature scans were run on samples that were placed in a closed pan and weighed 10–15 mg for ten successive heating and cooling

cycles. All samples were brought to thermal equilibrium at the starting temperature, held for 10 min, followed by heating the samples to the final temperature at a 5 °Cmin^{-1} heating rate and holding for 10 min. Finally, the samples were cooled to the starting temperature at a 5 °Cmin^{-1} cooling rate. Thermogravimetric (TG) analysis of the samples were achieved from 20 to 800 °C at 10 °Cmin^{-1} under a dry nitrogen atmosphere purged at a rate 20 mLmin^{-1} by a SEIKO EXSTAR 6200 Model TG/DTA instrument.

Morphology and surface characteristics of all produced nanowebs were analyzed via Scanning Electron Microscope (SEM) using Philips XL 30 SFEG type SEM. To prepare the SEM samples, dried nanowebs were placed on standard mounts, 15 mm in diameter and 2 mm in depth, under vacuum and coated with a 1–2 nm thick conductive layer of gold to prevent charging during imaging. The diameter distributions of nanofibers and porosity fractions of nanowebs were obtained from the SEM images with 10 k magnification via "ImageJ-DiameterJ" software [44].

3 Results and Discussion

3.1 The structural and thermal characterizations of PEG-g-PAN copolymers

3.1.1 FTIR results of PEG-g-PAN copolymers

Fig. 3 illustrates the full FTIR spectra of the PEG-g-PAN copolymers as well as that of PAN control. All distinctive bands of PEG, MA and PAN chains were observed in the expected regions of the FTIR spectra of the synthesized copolymers with some slight shifts, indicating successful grafting of PEG-MA macromonomers and AN chains.

The characteristic transmission bands at 2243 cm^{-1} and 1345–1343 cm^{-1} in the FTIR spectrum of PAN control, assigned to the stretching and bending vibrations of nitrile (–C≡N) groups, respectively, also appeared in the FTIR spectra of all PEG-g-PAN copolymers and confirmed the formation of PAN chains in the structure of the copolymers. The broad band at 3455–3415 cm^{-1} and the medium band at 1635–1622 cm^{-1} were associated with stretching (ν_1) and bending (ν_2) vibrations of –OH groups of PEG, correspondingly; whereas the bands, related with stretching vibrations of ether groups (–

$H_2C–O–CH_2–$) of PEGs and carboxyl group (O–C=O) of MA, appeared as strong and medium bands at 1281 cm^{-1}, 1243 cm^{-1} and 1148–1100 cm^{-1}. All these bands were characteristic indicators for the presence of PEG-MA chains in the structure of synthesized copolymers. Meanwhile, the strong bands at 2940–2916 cm^{-1}, 2854–2848 cm^{-1}, 958–947 cm^{-1} and 844–842 cm^{-1} were the signs of the stretching vibrations of $–CH_3$, $–CH_2$, –CH groups of PEG and PAN chains [21, 40].

3.1.2 NMR results of PEG-g-PAN copolymers

1H-NMR and 13C-NMR spectra of PEG1500-g-PAN, PEG2000-g-PAN, PEG4000-g-PAN, PEG10000-g-PAN and PEG35000-g-PAN with their peak assignments are shown respectively in Fig. 4 and 5. They all exhibited characteristic signals of PEG-MA and PAN segments. The H signals at about 1.8 ppm and between 2.0–3.2 ppm (labeled as d) belonged to the alkyl protons of PAN backbone [45]. The peak at about 2.5 ppm referred to the solvent DMSO-d_6.The H signals between 3.3–3.6 ppm (labeled as a and b) corresponded to the alkyl protons which were next to the ether ($–H_2C–O–CH_2–$) groups of PEG units [46]. The rest of methylene-chain hydrogen signals in the 1H-NMR spectra were located between 1.2 and 1.4 ppm [47].

The 13C-NMR spectra of all the synthesized copolymers displayed the main resonances of the acrylonitrile units of PAN as well as those of the ether and carboxyl units of PEG-MA oligomers.The signals of C between 26–29 ppm, 31–34 ppm belonged to the $–CH_2$ groups of PAN (labeled as c and d) and the signals around 120 ppm corresponded to –C≡N units of PAN backbones (labeled as e).The signals at 60–61 ppm characterized the terminal CH_2 unit next to the –OH units at the end of PEG chains (labeled as a). The C signals at 70–73 ppm referred to the $–H_2\mathbf{C}–\mathbf{O}–\mathbf{C}H_2–$ units of PEG chains (labeled as a and b). 1H-NMR and 13C-NMR results, which are in good agreement with FTIR results, approve successful

grafting of PEG-MA oligomers onto PAN backbone for all of the PEG-g-PAN copolymers [46] and [47].

3.1.3 DSC results of PEG-g-PAN copolymers

The thermal responses of PEG1500-g-PAN, PEG2000-g-PAN, PEG4000-g-PAN, PEG10000-g-PAN and PEG35000-g-PAN during 2nd and 10th heating and successive cooling cycles in DSC analyses, compared to those of the corresponding PEG oligomer and PEG-MA macromonomer are summarized in Table 4.

As illustrated in Table 4, the solid-liquid phase change enthalpies of PEG1500, PEG2000, PEG4000, PEG10000 and PEG35000 were measured 160 Jg^{-1}, 183 Jg^{-1}, 197 Jg^{-1}, 192 Jg^{-1} and 180 Jg^{-1} correspondingly during the 2nd heating cycle. Those latent heat of fusion values were all quite large, and the PEGs selected were accordingly suitable to produce a variety of new heat storage and release products. The observed decreases in enthalpy values of PEG-MA esters were associated with relatively reduced percentages of the PCMs in their macromonomers; however, their phase change enthalpies occurred still close to those of PEGs (76%–90% of them), implying the successful transesterification reaction between PEG and MAH chains [22]. The slight shifting of the phase transitions to lower temperature intervals with respect to the corresponding PEG oligomers was related to the decreasing physical attractions between PEG-MA chains.

The solid-solid phase change enthalpies during heating processes of PEG1500-g-PAN, PEG2000-g-PAN, PEG4000-g-PAN, PEG10000-g-PAN and PEG35000-g-PAN reached to the values of 88 Jg^{-1}, 70 Jg^{-1}, 126 Jg^{-1}, 100 Jg^{-1} and 93 Jg^{-1} in the temperature intervals of 43–56 ^{o}C, 40–54 ^{o}C, 53–61 ^{o}C, 55–65 ^{o}C and 56–64 ^{o}C, corresponding to 55%, 38%, 64%, 52% and 52% of the enthalpy values of the PEG oligomers. Those enthalpy values were comparatively great, indicative of the successful synthesis of PEG-g-PAN copolymers and their suitability for thermal energy storage applications. The onset, peak and end temperatures for the heating cycles of PEG-g-PAN samples slightly shifted to the lower temperatures compared to those of PEG and PEG-MA chains (see Table 4). These

observations can be attributed to a decrease in the extent of hydrogen bonding between the ether oxygen ($H_2C–O–CH_2$) and hydroxyl groups of PEGs in the neighboring chains of PEG-g-PAN copolymers [14], [20] and [48]. During cooling cycles, the shifts towards lower solid-solid phase transition temperature intervals for all of the PEG-g-PAN copolymers were most likely due to postponing of phase change from amorphous or semi-crystalline configuration to ordered crystalline configuration [20]. After ten heating and cooling cycles, the phase transition temperature intervals and enthalpies of solid-solid phase transition for the PEG-g-PAN copolymer samples remained almost constant, specifying thermal cycling stability of the synthesized PEG-g-PAN copolymers that is essential for their long-term use as PCM.

3.1.4 TG results of PEG-g-PAN copolymers

The TG thermograms of PEG1500-g-PAN, PEG2000-g-PAN, PEG4000-g-PAN, PEG10000-g-PAN, PEG35000-g-PAN and PAN control are displayed in Fig.6. The thermal decompositions of all the copolymers occurred mainly in one step, starting at 280^{o}C and ending at 432–460°C. As seen from Fig 6, the onset and end temperatures of thermal decomposition curves of the copolymers raised gradually as the chain length of PEG increased from PEG1500 to PEG35000 in the structure of PEG-g-PAN copolymers. The mass loss, due to the cyclization of the nitrile groups and the evolution of small molecules such as NH_3 and HCN, started at 380–398°C [49] and [50]. Then the thermal decomposition reactions speeded up by the evolution of PEG oligomers from the uncyclized portion of the copolymer, and ended at 432–460°C [22]. When the TG curves of PEG-g-PAN copolymers were compared with that of PAN control, the decompositions of PEG-g-PAN copolymers took place at higher temperatures with respect to that of PAN control, pointing the existence of covalent bonds between PEG-MA chains and PAN chains. The residues of PEG-g-PAN copolymers as well as that of PAN control at 510 ^{o}C were related to non-volatile hard segment of the polymer chains [49] so that 13–27% residues of PEG-g-PAN copolymers were less than 54% residue of PAN control,

reminding the presence of PEG-MA chains in PEG-g-PAN copolymers. The TG results are in good agreement with the DSC results and confirm the achievement of a substantial thermal stability for the PEG-g-PAN copolymers which were successfully synthesized as SSPCM

3.2 The structural and thermal characterizations of electrospun PEG-g-PAN nanowebs

3.2.1 Physicochemical properties of the solutions

The kinematic viscosities of the shell solutions lied in the range of 137–199 m^2s^{-1} and their surface tensions ranged between 0.037 and 0.047 Jm^{-2}; thus showing the tendency of a slight increase with increasing chain length of PEG groups in PEG-g-PAN copolymers (See Table 5). All solutions presented electrical conductivity between 32 and 65 μScm^{-1} sufficient for processing them. These characteristics of the shell solutions as well as the applied electrospinning parameters were all found suitable for the electrospinnability of the nanofibers.

3.2.2 Morphological properties of the nanowebs

Fig.7 a to f show SEM images of 6PAN and A1–A5 nanowebs given together with the corresponding histograms for diameter distributions of their nanofibers. The surfaces in the SEM images are characterized by randomly oriented nanofibers in conjunction with the several nanoscale pore areas of still air. The fractional porosity of the nanowebs are obtained between 0.49 and 0.60 as in many of the textile surfaces. Mainly the cylindrical nanofiber formation appears in the SEM images, regarded as smooth and beadless surfaces so that the uniformity along the fiber is maintained. Histograms given for the diameter distributions of the nanofibers indicate that fineness of the fibers lies in the nanoscale and positively skewed, therefore, the weighted averages of nanofiber diameters are centered at about 200 nm; for instance, the weighted average nanofiber diameter of A1 is obtained as 186 nm with the standard deviation of 121 nm and that of A2 is 229 nm with the standard deviation of 209 nm. As seen in Fig.7, the fiber diameters of A1, A2, A3, A4 and A5,

ranging in 175–277 nm, are less than that of 6PAN (290 nm) referable to their lower viscosities compared to 6PAN [32].

Fig. 8 and Fig. 9 demonstrate the SEM images of the longitidunal sections of nanofibers contained in A4 and A5, respectively. As clearly distinguished from the SEM images, nonofibers are continuous 1D structures made up of the PEG-g-PAN and PAN shell and hollow core. The thickness of the shell of A4 type nanofiber, shown in Fig.8.b, is about one fifth of the total fiber diameter, implying that air flow through the inner spinneret during electrospinning process prevented the collapse of nanofibers and enhanced hollow nanofiber formation with cylindrical geometry. The thickness of the shell of A5 type nanofiber, shown in Fig.9.b, is only about one tenth of the total fiber diameter as an evidence of ultra fine fiber structure entrapping huge amount of still air.

3.2.3 FTIR transmission spectra of the nanowebs

The FTIR transmission spectra of the A1–A5 and 6PAN nanowebs are given in Fig.10. The IR spectra of A1, A2, A3, A4, A5 presented all the distinctive bands of PEG-g-PAN and PAN, emphasizing that no phase separation or structural changes occurred in the mixture of PEG-g-PAN and PAN during electrospinning.

3.2.4 DSC measurements of the nanowebs

The thermal responses of A1–A5 during 2^{nd} and 10^{th} heating and successive cooling cycles in DSC analyses are shown in Fig.11. It was evidently observed from Fig.11 that the phase transition behaviour of electrospun A1, A2, A3, A4 and A5 nanoweb samples substantially coincided with those of the corresponding PEG-g-PAN copolymers, suggesting that the nanofiber formation from the shell mixtures of PEG-g-PAN and PAN was achieved successfully without any alteration in the structural and thermal properties of PEG-g-PAN copolymers (see also Table 4). The DSC graphs of A1–A5 in Fig.11 were well defined single curves, both in heating and cooling cycles. The DSC results verified a good extent of

electrospun nanoweb formation from PEG-g-PAN copolymers, which were also in good agreement with FTIR results.

The yields of A1–A5 nanowebs in terms of their heat capacities were all notable, corresponding to 38%, 40%, 47%, 80% and 68% of the associated PEG-g-PAN copolymer. In addition, after ten heating and cooling cycles, practically no difference in DSC results of each of the nanoweb samples was observed, implying that all hollow fiber nanowebs retain their thermal stability during thermal cycling.

Conclusion

In this study, a series of PEG-g-PAN copolymers with various molecular weights of PEG were synthesized as novel solid-solid PCM via two step free radical copolymerization, and then nanowebs composed of hollow nanofibers of as synthesized PEG-g-PAN copolymers were fabricated by coaxial electrospinning. FTIR, NMR, DSC and TG analyses revealed that chemically and thermally stable PEG-g-PAN copolymers were successfully produced. While heating, all of the synthesized PEG-g-PAN copolymers, namely PEG1500-g-PAN, PEG2000-g-PAN, PEG4000-g-PAN, PEG10000-g-PAN and PEG35000-g-PAN, revealed solid-solid phase transition in the temperature intervals of 43–56 ^{o}C, 40–54 ^{o}C, 53–61 ^{o}C, 55–65 ^{o}C and 56–64 ^{o}C by absorbing heat of 88 Jg^{-1}, 70 Jg^{-1}, 126 Jg^{-1}, 100 Jg^{-1} and 93 Jg^{-1}, respectively. Those enthalpy values are comparatively great, indicative of the successful synthesis of PEG-g-PAN copolymers and their suitability for thermal energy storage applications for warm to hot environmental conditions.

As-spun nanowebs, produced from one to one mixture of 10% PEG-g-PAN and 6%PAN solutions, were all composed of hollow cylindrical ultrafine fibers with the average diameters ranging in 175–277 nm, where the entrapped still air within and between the hollow fibers could improve the thermal insulation properties of the nanowebs. The PEG-g-PAN nanowebs demonstrated repeatable solid-solid phase change with the heat storage

capacities varying between 35 and 75 Jg^{-1} at the same temperature interval with the corresponding PEG-g-PAN copolymers.

Conclusively, PEG-g-PAN copolymers and the electrospun nanowebs produced in this study can be promising dynamic thermal energy storage materials and can have convenient industrial applications in the fields such as the solar energy systems and solar panels, batteries, greenhouses and building envelopes as well as aerospace, automotive, defense, sport and casual textiles.

ACKNOWLEDGEMENT

This work was based on the research project TUBITAK 213M281, which was funded by the Scientific & Technical Research Council of Turkey (TUBITAK). We also thank Istanbul Kultur University for financial support.

References

1. Benson DK, Christensen CB, Burrows RW. New phase-change thermal energy storage materials for buildings. International Conference on Energy Storage for Building Heating and Cooling, Toronto, Canada, 1985.
2. Singh H, Talekar A, Chien WM, Shi R, Chandra D, Mishra A, Tirumala M, Nelson DJ. Continuous solid-state phase transitions in energy storage materials with orientational disorder-Computational and experimental approach, Energy 2015; **91:** 334–349, DOI:10.1016/j.energy.2015.07.130.
3. Wang X, Lu E, Lin W, Wang C, Micromechanism of heat storage in a binary system of two kinds of polyalcohols as a solid-solid phase change material, Energ Convers Manage 2000; **41**:135–144, DOI:10.1016/S0196–8904(99)00096–5.

4. Alkan C, Sarı A, Biçer A. Thermal energy storage by poly(styrene-co-p-stearoylstyrene) copolymers produced by the modification of polystyrene. J Appl Polym Sci 2012; **125:** 3447–3455, DOI: 10.1002/app. 36527.

5. Tong B, Tan ZC, Liu RB, Meng CG, Zhang JN. Thermodynamic investigation of a solid–solid phase change material: 2-amino-2-methyl-1,3-propanediol by calorimetric methods. Energ Convers Manage 2010; **51:**1905–1910, DOI:10.1016/j.enconman.2010.02.021.

6. Sarı A, Alkan C, Biçer A, Karaipekli A, Synthesis and thermal energy storage characteristics of polystyrene-graft-palmitic acid copolymers as solid-solid phase change materials. Sol Energy Mater Sol Cell 2011; **95:** 3195–3201, DOI :10.1016/j.solmat.2011.07.003.

7. Shi H, Li J, Jin Y, Yin Y, Zhang X. Preparation and properties of poly(vinyl alcohol)-g-octadecanol copolymers based solid-solid phase change materials. Mater Chem Phys 2011; **131:**108–112, DOI:10.1016/j.matchemphys.2011.07.074.

8. Sarı A, Alkan C, Lafçı Ö. Synthesis and thermal properties of poly(styrene-co-ally alcohol)-graft-stearic acid copolymers as novel solid–solid PCMs for thermal energy storage. Sol Energy 2012; **86:**2282–2292, DOI:10.1016/j.solener.2012.04.018

9. Guo J, Xiang H, Wang Q, Hu C, Zhu M, Li L. Preparation of poly(decaglycerol-co-ethylene glycol) copolymer as phase change material. Energ Buildings 2012; **48:** 206–210, DOI:10.1016/j.enbuild.2012.01.035.

10. Zang YN, Ding EY. Energy storage properties of phase change materials prepared from PEG/CPP. Chinese Chem Lett 2005; **16(10):** 1375–1378.

11. Ding E, Jiang Y, Li G. Comparative studies of the structures and transition characteristics of cellulose diacetate modified with polyethylene glycol prepared by chemical bonding and physical blending methods. J Macromol Sci B 2001; **40(6):** 1053–1068, DOI:10.1081/MB–100107801.

12. Jiang Y, Ding E, Li G. Study on transition characteristics of PEG/CDA solid-solid phase change materials. Polymer 2002; **43(1):** 117–122, DOI:10.1016/S0032–3861(01)00613–9.

13. Sarı A, Alkan C, Biçer A. Synthesis and thermal properties of polystyrene–graft–PEG copolymers as new kinds of solid-solid phase change materials for thermal energy storage. Mater Chem Phys 2012; **133(1):** 87–94, DOI:10.1016/j.matchemphys.2011.12.056.

14. Cao Q, Liu P. Hyperbranched polyurethane as novel solid–solid phase change material for thermal energy storage. Eur Polym J 2006; **42(11):** 2931–2939, DOI:10.1016/j.eurpolymj.2006.07.020.

15. Su J, Liu P. A novel solid-solid phase change heat storage material with polyurethane block copolymer structure. Energ Convers Manage 2006; **47(18–19)**: 3185–3191, DOI:10.1016/j.enconman.2006.02.022.

16. Li Y, Liu R, Huang Y. Synthesis and phase transition of cellulose-graft-poly(ethylene glycol) copolymers. J Appl Polym Sci 2008; **110:** 1797–1803, DOI: 10.1002/app.28541.

17. Zhang M, Na Y, Jiang Z. Preparation and properties of polymeric solid–solid phase change materials of polyethylene glycol (PEG)/poly (vinyl alcoho1) (PVA) copolymers by graft copolymerization. Chem J Chinese U 2005; **26:**170–174.

18. Hu J, Yu H , Chen Y, Zhu M. Study on Phase-Change Characteristics of PET-PEG Copolymers. J Macromol Sci B 2006; **45(4):** 615–621, DOI: 10.1080/00222340600770210

19. Kuru A, Alay Aksoy S. Cellulose–PEG grafts from cotton waste in thermo–regulating textiles. Text Res J 2014; **84:** 337–346, DOI: 10.1177/0040517513494251.

20. Li W, Ding E. Preparation and characterization of cross–linking PEG/MDI/PE copolymer as solid–solid phase change heat storage material. Sol Energy Mater Sol Cell 2007; **91(9):** 764–768, DOI:10.1016/j.solmat.2007.01.011

21. Alkan C, Günther E, Hiebler S, Ensari ÖF, Kahraman D. Polyurethanes as solid–solid phase change materials for thermal energy storage. Sol Energy 2012; **86(6):** 1761–1769, DOI:10.1016/j.solener.2012.03.012.

22. Zhi SH, Deng R, Xu J, Wan LS, Xu ZK. Composite membranes from polyacrylonitrile with poly(N,N-dimethylaminoethyl methacrylate)-grafted silica nanoparticles as additives. React Funct Polym 2015; **86:** 184–190, DOI:10.1016/j.reactfunctpolym.2014.09.004.

23. Guo J, Xie P, Zhang X, Yu CF, Guan FC, Liu YF. Synthesis and characterization of graft copolymer of polyacrylonitrile–g–polyethylene glycol–maleic acid monoester macromonomer. J Appl Polym Sci 2014, **131:** 1–6, DOI: 10.1002/app.40152

24. Mu S, Guo J, Gong Y, Zhang S, Yu Y. Synthesis and thermal properties of poly(styrene–co–acrylonitrile)–graft–polyethylene glycol copolymers as novel solid–solid phase change materials for thermal energy storage. Chinese Chem Lett 2015; **26(11):** 1364–1366, DOI:10.1016/j.cclet.2015.07.013.

25. Mu S, Guo, J, Qi, S, Zhang, B, Zhang, H, Yu, Y Synthesis and characterization of poly(acrylonitrile–co–itaconate)–graft–PEG copolymers as novel solid–solid phase change materials for thermal energy storage. Chem J Chinese U 2015, **36(12)**: 2557–2562. DOI: 10.7503/cjcu20150655.

26. Vigo TL, Frost CM. Temperature-adaptable hollow fibers containing polyethylene glycols. J Coated Fabrics 1983; **12**:243–254, DOI: 10.1177/152808378301200405.

27. Vigo TL, Frost CM. Temperature adaptable fabrics. Text Res J 1985; **55**: 737–743, DOI: 10.1177/004051758505501205.

28. Zhang XX, Wang XC, Hu L. Spinning and properties of PP/PEG composite fibers for heat storaging and thermo regulating. J Tianjin I Text Sci Technol 1999; **18(1):**1–4.

29. Zhang XX, Wang XC, Tao XM, Yick KL. Structures and properties of wet spun thermo-regulated polyacrylonitrile-vinylidene chloride fibers. Text Res J 2006; **76:**351–359, DOI: 10.1177/0040517506061959.

30. Hu J, Yu H, Chen Y, Zhu M. Study on phase-change characteristics of PET–PEG co-polymers. J Macromol Sci B 2006; **45(4):**615–621, DOI: 10.1080/00222340600770210.

31. Meng Q, Hu J. A temperature–regulating fiber made of PEG–based smart co-polymer. Sol Energy Mater Sol Cell 2008; **92(10):**1245–1252, DOI: 10.1016/j.solmat.2008.04.027.

32. Chen C, Liu S, Liu W, Zhao Y, Lu Y. Synthesis of novel solid–liquid phase change materials and electrospinning of ultrafine phase change fibers. Sol Energy Mater Sol Cell 2012; **96:** 202–209, DOI: 10.1016/j.solmat.2011.09.057.

33. Chen C, Wang L, Huang Y. Electrospinning of thermo–regulating ultrafine fibers based on polyethylene glycol/cellulose acetate composite. Polymer 2007; **48(18):**5202–5207, DOI: 10.1016/j.polymer.2007.06.069.

34. Nguyen TTT, Park JS. Fabrication of electrospun nonwoven mats of polyvinylidene fluoride/polyethylene glycol/fumed silica for use as energy storage materials. J Appl Polym Sci 2011; **121:**3596–3603, DOI: 10.1002/app.34148.

35. Onder E, Sarier N. Chapter 2: Thermal Regulation Finishes For Textiles, in Functional Finishes For Textiles: Improving Comfort, Performance And Protection. Edited By R Paul, Woodhead Publishing Series in Textiles No.156, p.17-98, ISBN 0 85709 839 X ISBN-13: 978 0 85709 839 9 (print), 2015, 629 pp.

36. Hooftman G, Herman S, Schacht E. Review: poly (ethylene glycol)s with reactive endgroups. II. Practical consideration for the preparation of protein-PEG conjugates. J Bioact Compat Pol 1996; **11(2):**135–159, DOI: 10.1177/088391159601100205.

37. Zhang L, Guo J, You X, Liu Y, Yang L, Zhang B, Zhang S, Gong Y. Preparation and properties of P(AN-co-AM)-g-MAPEG phase-change nanofibers. High Perform Polym 2016; **22(2):**231–238, DOI: 10.1177/0954008315579111.

38. Asatekin A, Kang S, Elimelech M, Mayes AM. Anti-fouling ultrafiltration membranes containing polyacrylonitrile-graft-poly(ethylene oxide) comb copolymer additives. J Membrane Sci 2007; **298(1-2):**136–146, DOI: 10.1016/j.memsci.2007.04.011.

39. Nataraj SK, Yang KS, Aminabhavi TM. Polyacrilonitrile-based nanofibers – A state-of-the-art review. Prog Polym Sci 2012; **37:**487–513, DOI: 10.1016/j.progpolymsci.2011.07.001.

40. Yordem OS, Papila M, Menceloglu YZ. Effects of electrospinning parameters on polyacrylonitrile nanofiber diameter: An investigation by response surface methodology. Mater Design 2008; **29(1):**34–44, DOI: 10.1016/j.matdes.2006.12.013.

41. American Society for Testing and Materials. Standard Test Method for Kinematic Viscosity of Transparent and Opaque Liquids (and Calculation of Dynamic Viscosity). ASTM International, 2009.

42. Riba JR, Esteban B. A simple laboratory experiment to measure the surface tension of a liquid in contact with air. Eur J Phys 2014; **35(5)**:055003, DOI: 10.1088/0143-0807/35/5/055003.

43. Loscertales IG, Barrero A, Márquez M, Spretz R, Velarde-Ortiz R, Larsen G. Electrically forced coaxial nanojets for one-step hollow nanofiber design. J Am Chem Soc 2004; **126(17):** 5376–5377, DOI: 10.1021/ja049443j.

44. Hotaling NA, Bharti K, Kriel H, Simon Jr CG. Dataset for the validation and use of DiameterJ an open source nanofibre diameter measurement tool. Data in Brief 2015; **5:**13–22, DOI: 10.1016/j.dib.2015.07.012.

45. Minagawa M, Ute K, Kitayama T, Hatada K. Determination of stereoregularity of gamma-irradiation canal polymerized polyacrylonitrile by 1H 2D J-Resolved NMR

spectroscopy. Macromolecules 1994; **27(13):**3669–3671, DOI: 10.1021/ma00091a032.

46. Tang GP, Zeng JM, Gao SJ, Ma YX, Shi L, Li Y, Too HP, Wang S. Polyethylene glycol modified polyethylenimine for improved CNS gene transfer: effects of PEGylation extent. Biomaterials 2003; **24(13):**2351–2362, DOI: 10.1016/S0142-9612(03)00029-2.

47. Ozturk T, Yilmaz SS, Hazer B, Menceloglu YZ. ATRP of methyl methacrylate initiated with a bifunctional initiator bearing bromomethyl functional groups: Synthesis of the block and graft copolymers. J Polym Sci Pol Chem 2010; **48(6):** 1364–1373, DOI: 10.1002/pola.23898.

48. Su JC, Liu PS. A novel solid–solid phase change heat storage material with polyurethane block copolymer structure. Energ Convers Manage 2006; **47:**3185–3191, DOI: 10.1016/j.enconman.2006.02.022.

49. Xue TJ, Mckinney MA, Wilkie CA. The thermal degradation of polyacrylonitrile. Polym Degrad Stabil 1997; **58(1):** 193–202, DOI: 10.1016/S0141-3910(97)00048-7.

50. Rahaman, MSA, Ismail AF, Mustafa A. A review of heat treatment on polyacrylonitrile fiber. Polym Degrad Stabil 2007; **92(8):**1421–1432, DOI: 10.1016/j.polymdegradstab.2007.03.023.

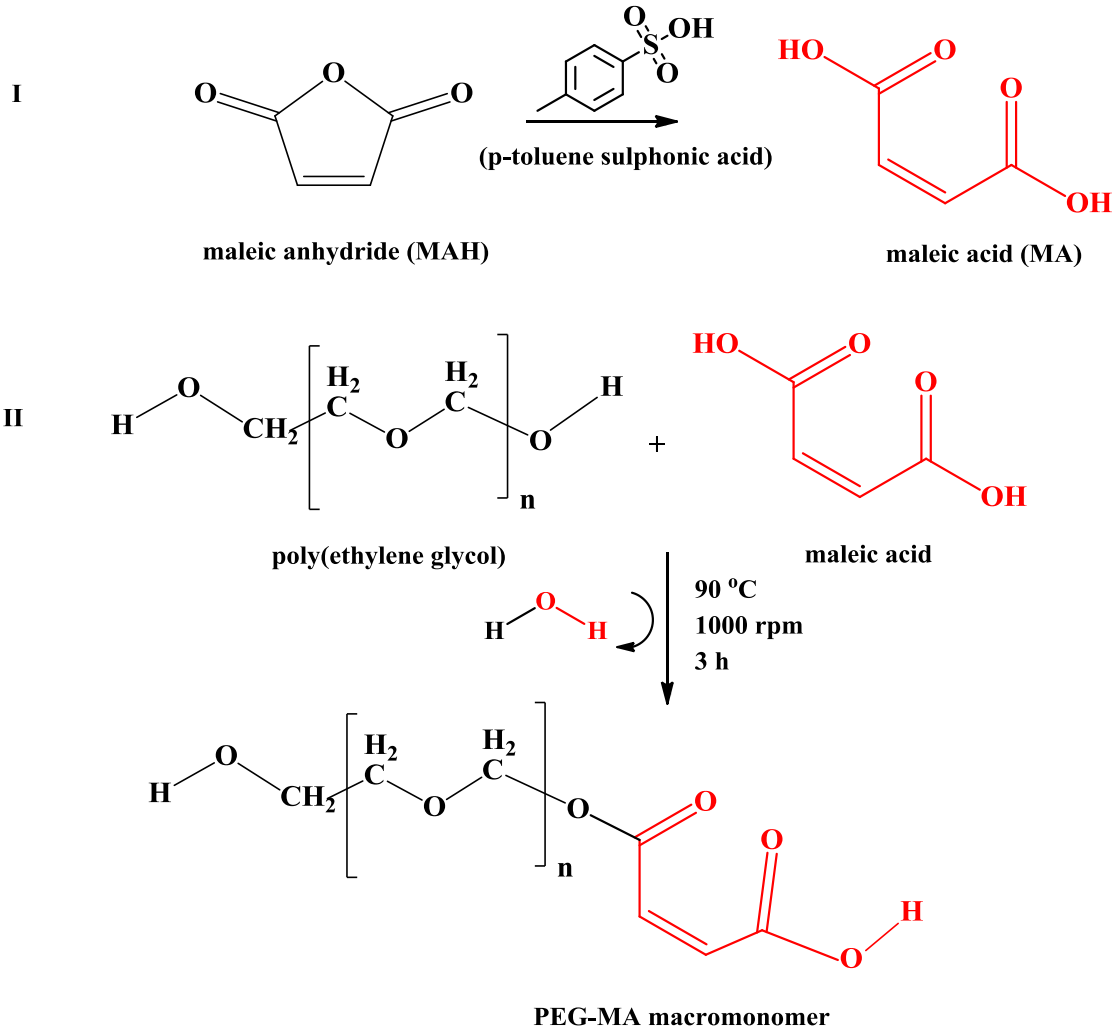

Figure 1. The transesterification reaction between a PEG oligomer and MAH to synthesize PEG-MA macromonomer.

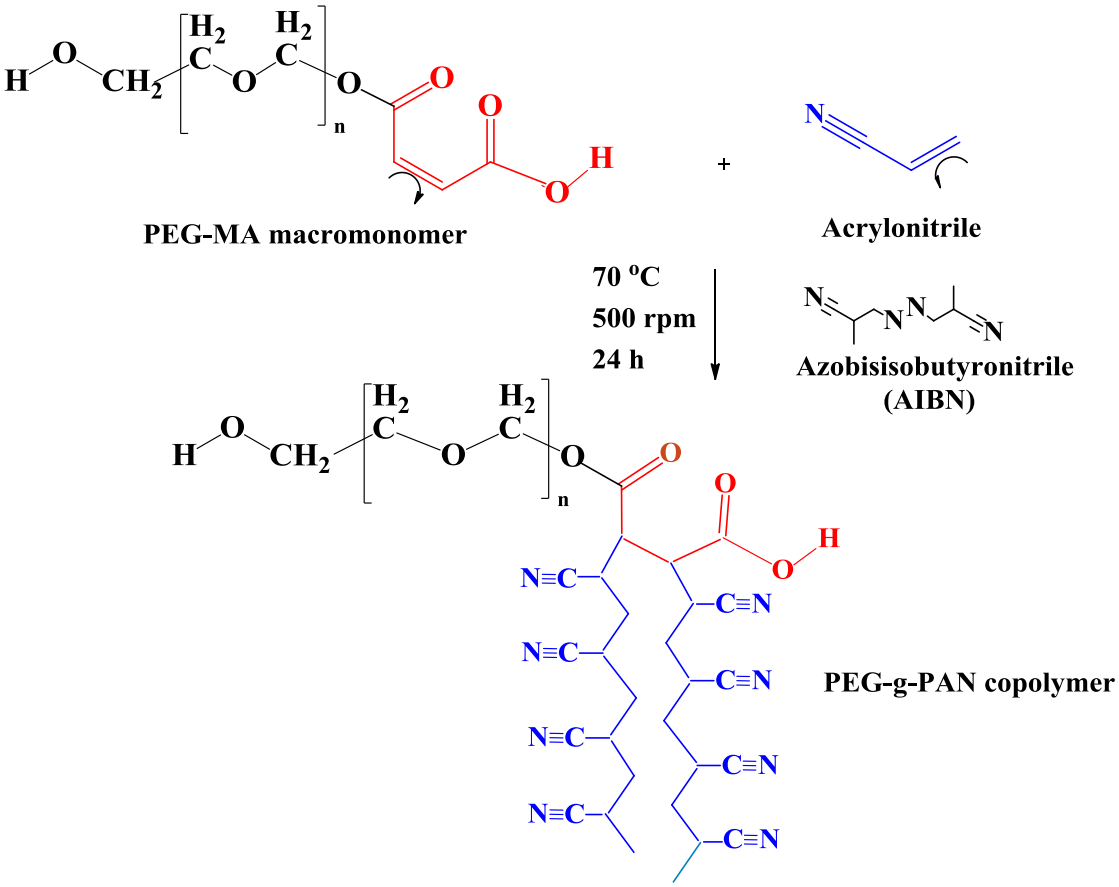

Figure 2. Grafting of PEG-MA with AN by a free radical polymerization.

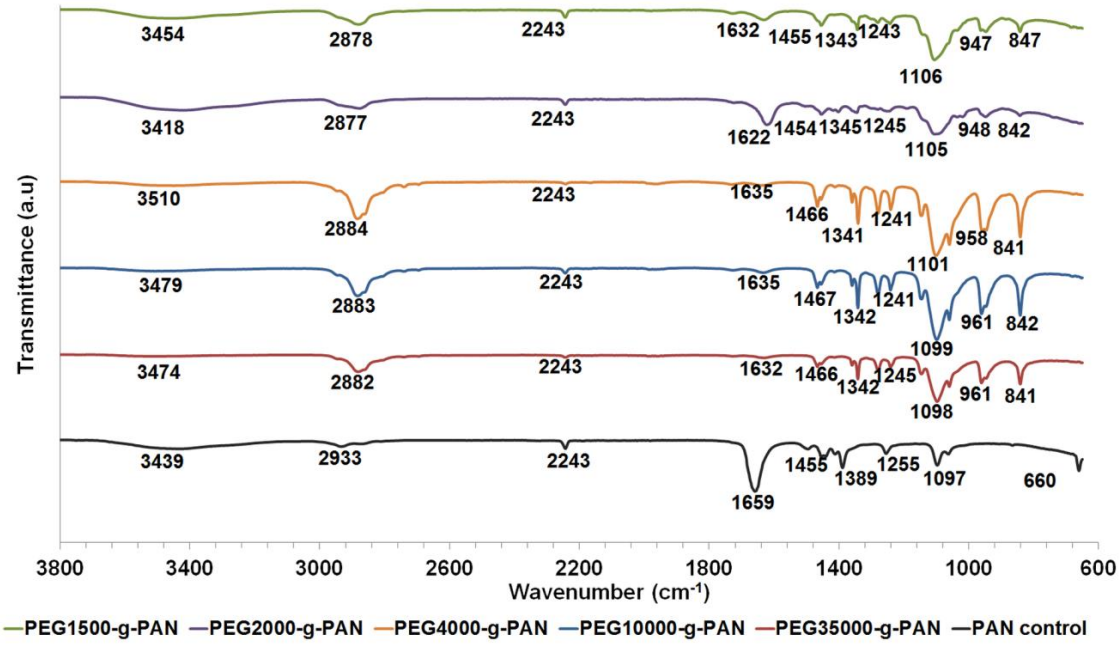

Figure 3. FTIR transmission spectra of PEG1500-g-PAN, PEG2000-g-PAN, PEG4000-g-PAN, PEG10000-g-PAN and PEG35000-g-PAN copolymers in comparison with PAN control.

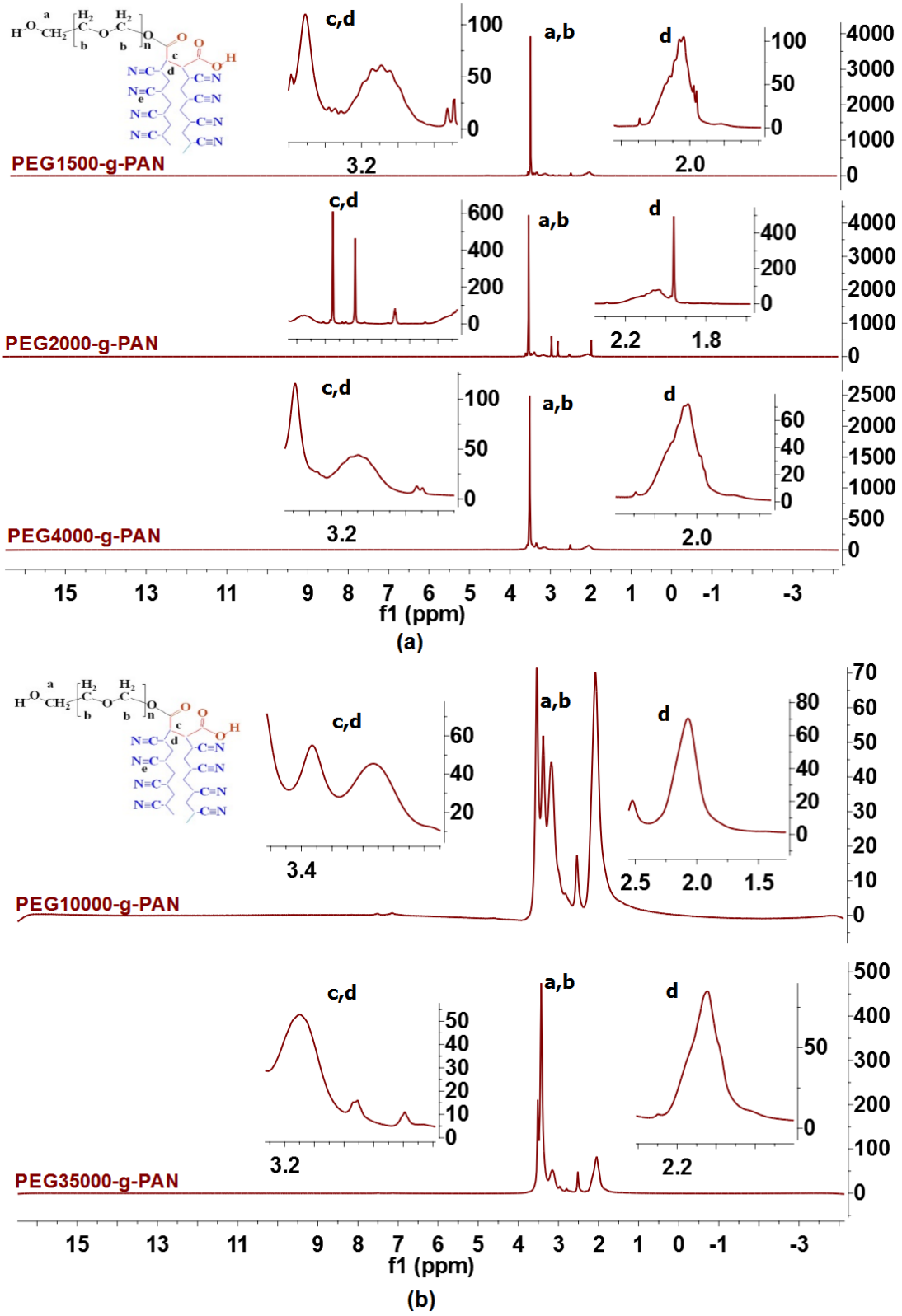

Figure 4. 1H-NMR spectra of: a)PEG1500-g-PAN, PEG2000-g-PAN and PEG4000-g-PAN; b) PEG10000-g-PAN and PEG35000-g-PAN copolymers.

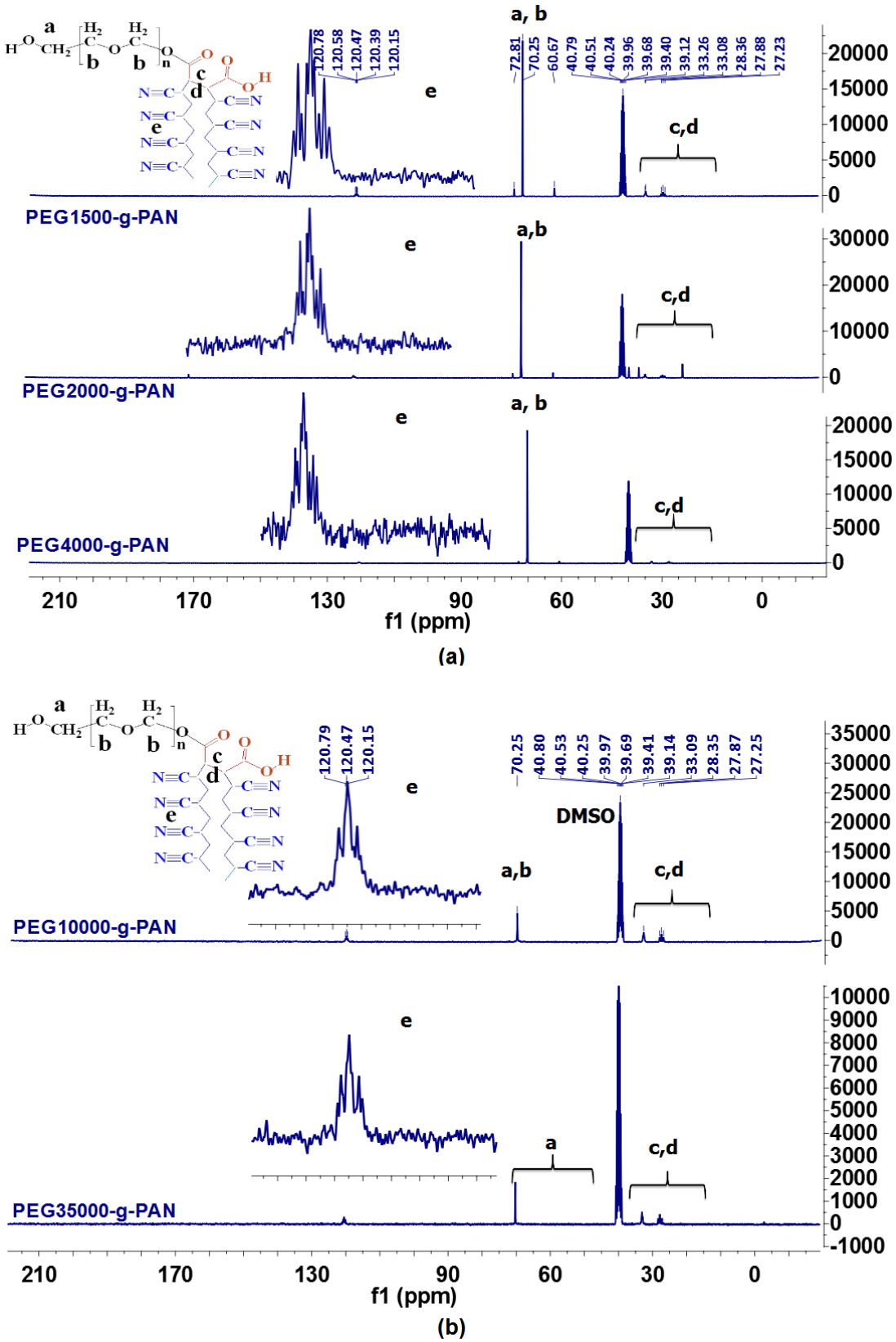

Figure 5. 13C-NMR spectra of: a)PEG1500 -g-PAN, PEG2000-g-PAN and PEG4000-g-PAN; b) PEG10000-g-PAN and PEG35000-g-PAN copolymers.

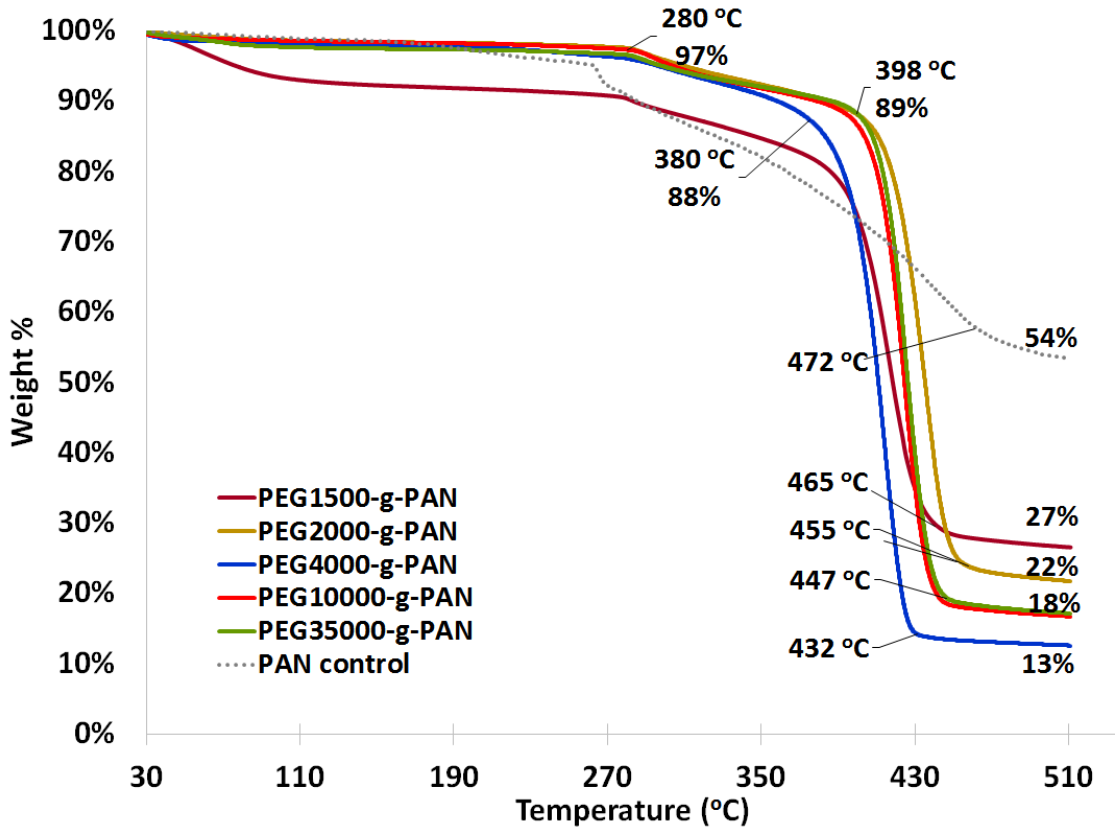

Figure 6. The TG thermograms of PEG1500-g-PAN, PEG2000-g-PAN, PEG4000-g-PAN, PEG10000-g-PAN, PEG35000-g-PAN and PAN control.

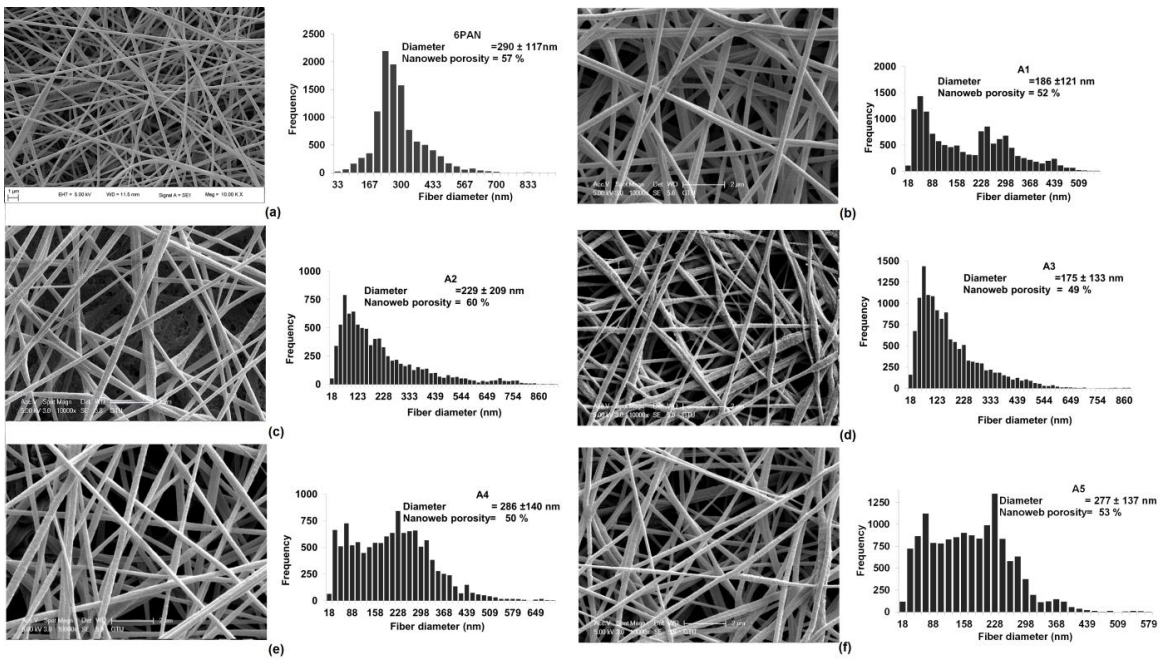

Figure 7. The SEM images (x10 k), fiber diameter distributions and porosity percentages of: a) 6PAN; b) A1; c) A2; d) A3; e) A4; and f) A5.

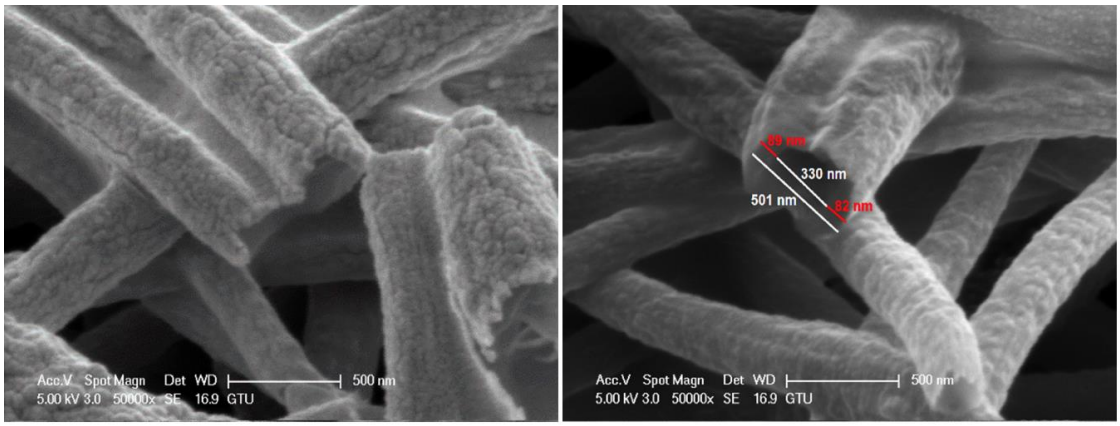

Figure 8. The SEM images of the longitudinal sections of A4 type nanofibers (x50 k)

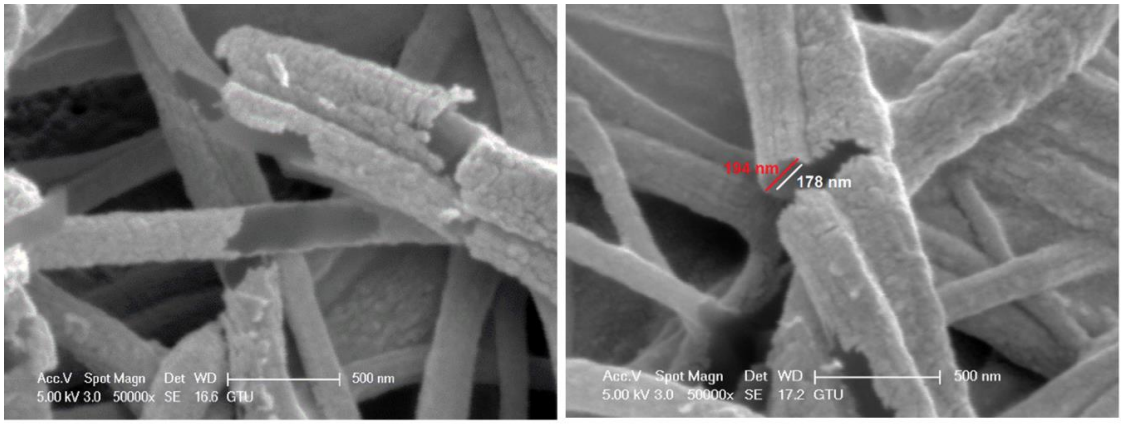

Figure 9. The SEM images of the longitudinal section of A5 type nanofibers (x50 k).

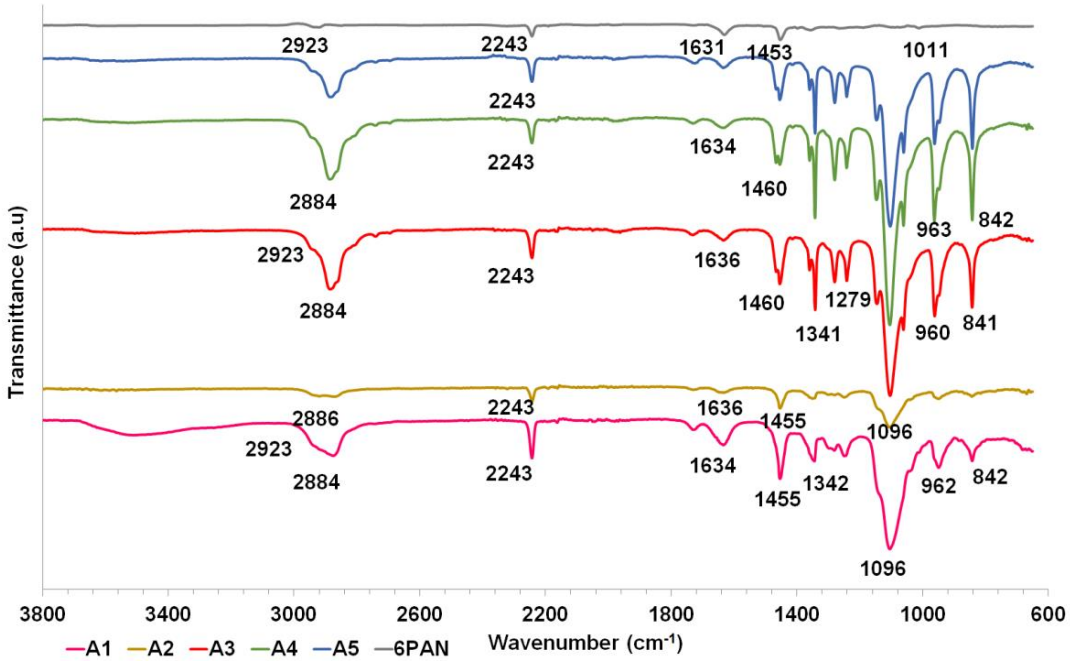

Figure 10. FTIR transmission spectra of A1, A2, A3, A4, A5 nanowebs and 6PAN nanoweb.

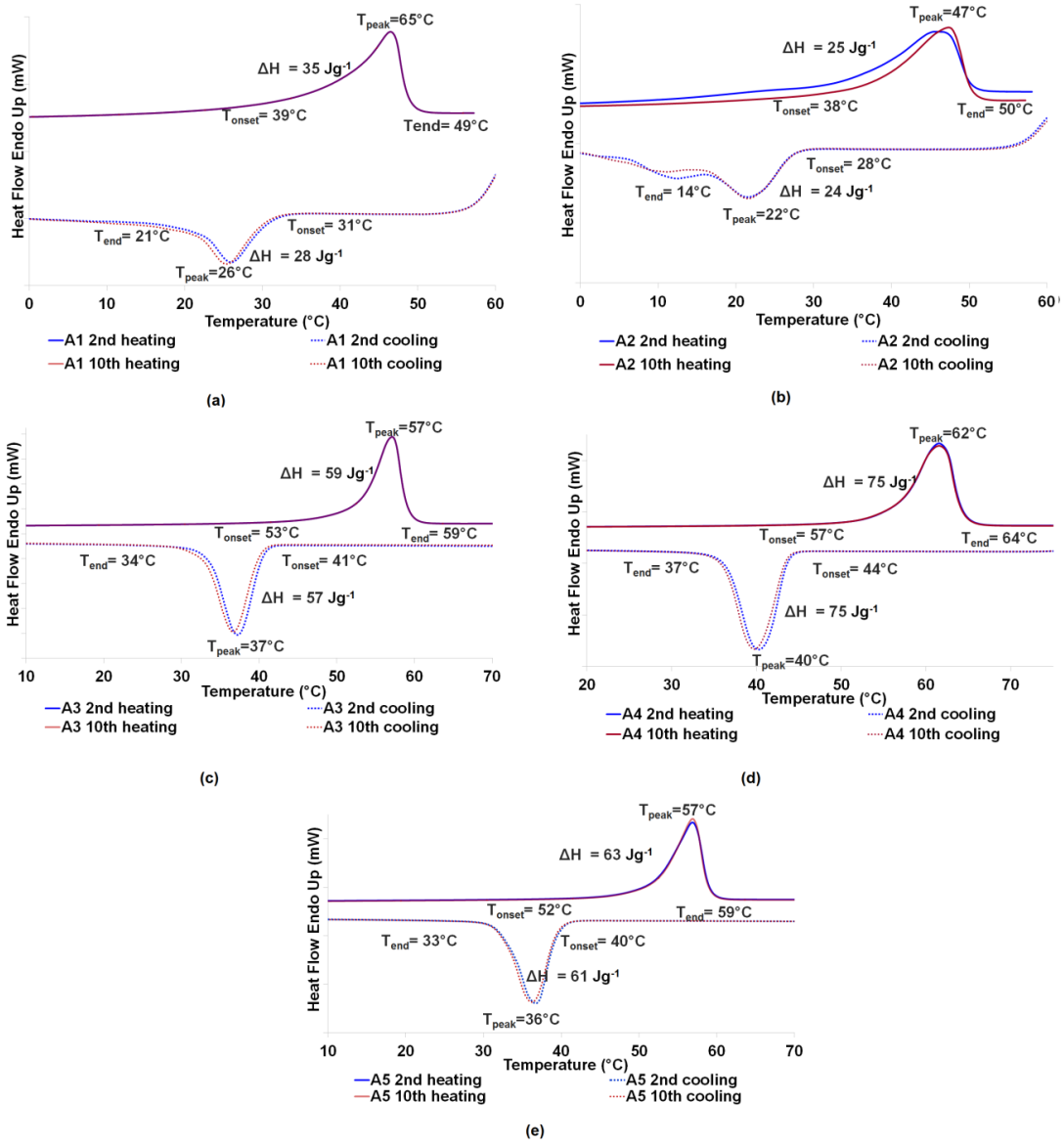

Figure 11. DSC curves of: a) A1; b) A2; c) A3; d) A4; and e) A5 nanowebs during 2nd and 10th heating and successive cooling cycles.

Table 1. Amounts of ingredients to produce PEG-MA macromonomers via transesterification reaction

	PEG oligomer (reactant)		MAH (reactant)	PTSA (catalyst)
Name of Macromonomer	**MW of PEG ($gmole^{-1}$)**	**Amount (mole)**	**Amount (mole)**	**Amount (g)**
PEG1500-MA	1500	$1.0x10^{-2}$	$1.0x10^{-2}$	0.320
PEG2000-MA	2000	$6.0x10^{-3}$	$6.0x10^{-3}$	0.252
PEG4000-MA	4000	$3.0x10^{-3}$	$3.0x10^{-3}$	0.246
PEG10000-MA	10000	$1.5x10^{-3}$	$1.5x10^{-3}$	0.300
PEG35000-MA	35000	$5.0x10^{-4}$	$5.0x10^{-4}$	0.350

Table 2. Amounts of ingredients to produce PEG-g-PAN copolymers by free radical polymerization

Name of Copolymer	**PEG-MA amount (g)**	**AN amount (g)**	**AIBN (catalyst) amount (g)**
PEG1500-g-PAN	5.00	5.00	0.05
PEG2000-g-PAN	5.00	5.00	0.05
PEG4000-g-PAN	5.00	5.00	0.05
PEG10000-g-PAN	5.00	5.00	0.05
PEG35000-g-PAN	5.00	5.00	0.05

Table 3. Optimized coaxial electrospinning parameters and conditions for the production of PEG-g-PAN and 6PAN nanowebs

	Components of a shell mixture (in DMAc)					Injector–Collector voltage difference
Specimen	**I. (50 mL)**	**II. (50 mL)**	**Core**	**Shell pump rate (mLh^{-1})**	**Core pump rate (mLh^{-1})**	**(kV)**
6PAN	-	6%PAN	Air	0.03	0.01	14.0
A1	10% PEG1500-g-PAN	6%PAN	Air	0.03	0.01	19.0
A2	10% PEG2000-g-PAN	6%PAN	Air	0.03	0.01	18.0
A3	10% PEG4000-g-PAN	6%PAN	Air	0.03	0.01	18.0
A4	10% PEG10000-g-PAN	6%PAN	Air	0.03	0.01	18.0
A5	10% PEG35000-g-PAN	6%PAN	Air	0.03	0.01	18.0

Table 4. DSC characteristics of PEG oligomers, PEG-MA macromonomers and PEG-g-PAN copolymers for 2nd and 10th heating and subsequent cooling processes at the rate of 5 ºCmin^{-1} between 0 ºC and 80 ºC

	2nd Heating				2nd Cooling				10th Heating				10th Cooling			
Specimen	**T_o**	**T_p**	**T_e**	**ΔH>0 (Jg^{-1})**	**T_o**	**T_p**	**T_e**	**ΔH<0 (Jg^{-1})**	**T_o**	**T_p**	**T_e**	**ΔH>0 (Jg^{-1})**	**T_o**	**T_p**	**T_e**	**ΔH<0 (Jg^{-1})**
PEG1500	44	54	58	**160**	28	21	17	**158**	44	54	58	**160**	28	21	17	**158**
PEG1500-MA	42	52	57	**134**	24	19	13	**128**	42	52	57	**134**	26	20	14	**129**
PEG1500-g-PAN	**43**	**52**	**56**	**88**	**24**	**21**	**16**	**90**	**44**	**52**	**57**	**88**	**24**	**21**	**16**	**91**
PEG2000	51	58	61	**183**	33	27	23	**182**	51	58	61	**182**	33	27	22	**180**
PEG2000-MA	44	53	54	**139**	36	31	28	**140**	44	53	54	**139**	36	31	28	**140**
PEG2000-g-PAN	**40**	**47**	**54**	**70**	**27**	**21**	**16**	**70**	**40**	**47**	**54**	**70**	**27**	**21**	**16**	**70**
PEG4000	53	59	65	**197**	38	32	28	**193**	55	60	65	**199**	38	33	28	**197**
PEG4000-MA	53	59	62	**160**	35	29	22	**155**	54	59	62	**160**	33	27	22	**155**
PEG4000-g-PAN	**53**	**58**	**61**	**126**	**36**	**32**	**28**	**125**	**54**	**59**	**61**	**126**	**36**	**32**	**28**	**125**
PEG10000	62	67	70	**192**	45	41	37	**180**	62	67	70	**192**	45	41	37	**180**
PEG10000-MA	60	65	68	**161**	45	39	33	**158**	60	65	68	**160**	44	39	35	**159**
PEG10000-g-PAN	**55**	**62**	**65**	**100**	**41**	**37**	**32**	**98**	**55**	**62**	**65**	**100**	**41**	**38**	**32**	**98**
PEG35000	62	68	72	**180**	47	42	37	**181**	64	68	72	**186**	48	43	40	**185**
PEG35000-MA	60	64	66	**161**	42	36	32	**160**	60	64	67	**161**	41	37	33	**158**
PEG35000-g-PAN	**56**	**61**	**64**	**93**	**44**	**40**	**36**	**90**	**56**	**61**	**64**	**93**	**44**	**40**	**36**	**90**

Table 5. Kinematic viscosity, surface tension and conductivity values of shell solutions prepared by mixing 10% PEG-g-PAN solutions with 6% PAN solution

Specimen	**Kinematic viscosity (η) m²s^{-1}**	**Surface tension (γ)(Jm^{-2})**	**Conductivity (μScm^{-1}) at 25 ºC**
6PAN	544	0.036	20
A1	137	0.037	65
A2	148	0.038	33
A3	156	0.043	28
A4	166	0.045	38
A5	199	0.047	32